Effective Width of Locally Post Buckled Welded Steel Plates in Concrete-Filled Tubular Thin-Walled Columns

Haitham. H. AlDaami
Civil Engineering , Babylon University/ College of Engineering

Abstract

The concept of elastic and plastic effective width is used to investigate the post-buckling behavior of welded steel plates compositing concrete-filled tubular thin-walled columns. The theoretical branch of this paper is presented by using the fiber element based on the nonlinearity of materials, while the experimental branch is represented by investigating the subject by many tested specimens. The effect of initial imperfections and residual stresses due to welding are considered in the analysis. New formulae are presented herein for the effective width equations depending on the experimental and the analytical parts. The results of both analytical and experimental approaches are compared and found in good agreement with difference not more than 6.6% for CFST column and about 15% for ST column.

Keywords: Tubular steel column, steel plates, concrete, post-buckling effective width, welding stresses.

خلاصة

تم استعمال فكرة العرض الفعال المرن و اللدن, لتحري السلوك لما بعد الانبعاج للألواح الحديدية المركبة للأعمدة الأنبوبية نحيفة الجدران المملوءة بالخرسانة. الجزء النظري من البحث شمل استعمال العنصر النسيجي معتمدا على العلاقات اللاخطية للمواد. بينما الجزء ألمختبري تضمن اختبار عدة نماذج. تأثير التشوه الأولي و الاجهادات المتبقية بسبب اللحام تم اعتمادها في التحليل . معادلات جديدة ثم تقديمها في البحث للعرض الفعال وذلك باعتماد على التحليل النظري و المختبري. النتائج لكلا التحريات النظرية والمختبرية ثم مقارنتها ووجد اختلاف مقبول بحدود اختلاف لا يتجاوز 6.6% للأعمدة الحديدية المملوءة بالخرسانة ونسبة بحدود 15% للأعمدة الحديدية.

1. Introduction

Thin-walled tubular steel columns filled with concrete core (Concrete-Filled Steel Tube **CFST**) have been used to support heavy loads in tall buildings. The uses of these building columns enable the rapid construction of structural elements. Design codes such as (Eurocode 4, 1994; AISC LRFD ,1999; ACI 318-05 ,2005) do not consider the effects of the plate local buckling on the ultimate strength of CFST columns. Tests on thin-walled CFST columns showed that thin steel plates might buckle award from the concrete core (Bridge *et al.*, 1995; Ge and Usami, 1999; Uy, 2000). The concrete (core) will behave in a more ductile behavior, and stress-strain of concrete will be improved (Liang, 2007).

The post-local buckling behavior and strength of rectangular plates subjected to edge compression force stresses has been investigated widely by several researchers such as (Liang and Uy , 2000; Liang *et al*, 2004, 2005).

The research work on the ultimate strength or effective width in the post buckling range is limited compared with pure compression. (Usami, 1982) has proposed an effective width formula as well as a strength formula of a plate in compression and bending, and applied the formula to compute the local buckling strength of eccentrically loaded box section members. (Nara *et al.* 1987) were introduce a paper on an elastic-plastic large displacement analysis including both welding type residual stresses and initial out-of-flatness taken into consideration, and proposed un interaction formula for the strength of plate in combined compression and bending. The interaction formula is useful to compute the strength of an isolated plate element; however, the strength of the whole cross section of a member (such as box section) could not be determined.

The fiber element method has been presented by (El-Tawil *et al.*1995) for the nonlinear analysis of concrete-encased composite columns under axial load and biaxial bending. (El-Tawil *et al.*, 1995) studied the ultimate strength and ductility of concrete-encased composite columns. (Lakshmi and Shanmugam , 2002) presented a semi-analytical model for analyzing CFST columns. (Liew *et al.*, 2001) developed an advanced analysis program for the nonlinear analysis of steel frames with composite beams. The effects of local buckling, however, have not been considered in nonlinear analysis methods for thin-walled CFST columns.

In this study, elastic and plastic effective width formulas are presented to investigate the post-buckling behavior of welded steel plates compositing concrete-filled tubular thin-walled columns. Nonlinear models for structural steel and confined concrete are used herein to represent the composite actions. Design formula for critical local buckling is employed in the analysis to account for local buckling effects. The effect of plates imperfection and the residual stresses due to welding of edges are considered in the analysis. The accuracy of the analysis is established by comparisons with experimental results made in this to monitor the actual behavior.

2. Fiber Element Analysis (Theoretical)

2.1 Constitutive Models for Steel

In the fiber element method, the composite section is discretized into many fiber elements. The fiber stresses for structural steels with residual stresses are calculated using the (Ramberg-Osgood formula 1943), which is expressed by:

$$\varepsilon_s = \frac{\sigma_s}{E_s}\left[1+\frac{3}{7}\left(\frac{\sigma_s}{\sigma_{0.7}}\right)^n\right] \tag{1}$$

where σ_s is the longitudinal stress in steel, ε_s is the longitudinal strain in steel, E_s is the Young's modulus of steel, $\sigma_{0.7}$ is the stress corresponding to $E_{0.7}= 0.7E_s$, and n is the knee factor that defines the sharpness of the stress-strain curve. The knee factor $n = 25$ is used in the fiber element analysis program to account for the isotropic strain hardening of steel sections (Liang, 2007). Figure 1, describe this nonlinear relation for the steel used in the experiments of the present study.

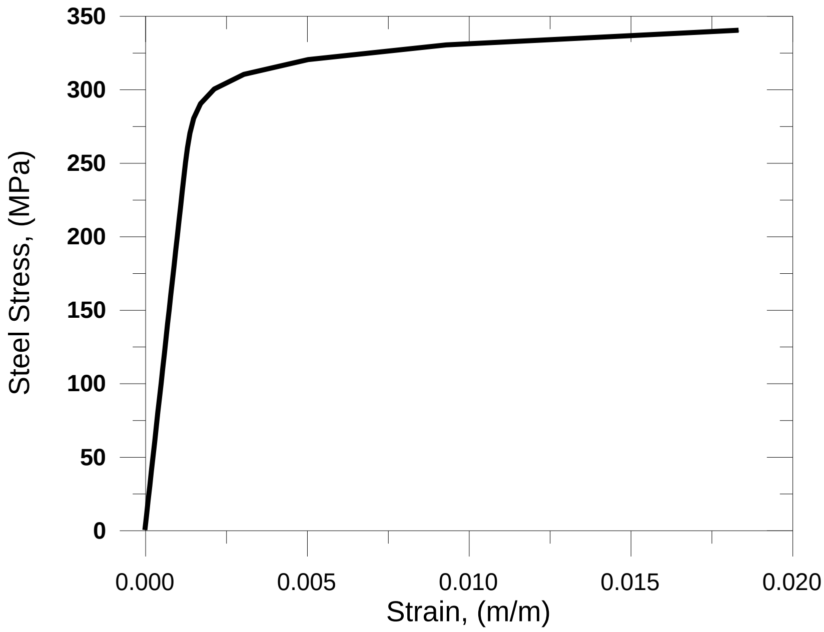

Figure (1): The Stress-Strain Constitutive Relation of Steel.

2.2 Constitutive Model for Concrete

It is assumed that the confinement effect increases only the ductility of the encased concrete in a CFST column but not its ultimate load (Tomii and Sakino, 1979). The general stress-strain curve for concrete in CFST columns is depicted in Figure 2. The curve is ploted for concrete with minimum cylinder compressive strength ($f_c^{'} = 32MPa$). The part OA of the stress-strain curve is modeled using the equation suggested by (Mander *et al.,* 1988) as:

$$\sigma_c = \frac{f_c^{'}\gamma\left(\frac{\varepsilon_c}{\varepsilon_c^{'}}\right)}{\gamma - 1 + \left(\frac{\varepsilon_c}{\varepsilon_c^{'}}\right)^{\gamma}} \qquad (2)$$

where σ_c is the longitudinal compressive concrete stress, $f_c^{'}$ is the compressive cylinder strength of concrete, ε_c is the longitudinal compressive concrete strain, $\varepsilon_c^{'}$ is the strain at $f_c^{'}$. The parameter γ is determined by:

$$\gamma = \frac{E_c}{E_c - \left(\frac{f_c^{'}}{\varepsilon_c^{'}}\right)} \qquad (3)$$

where E_c is the Young's modulus of concrete. The strain $\varepsilon_c^{'}$ is taken as 0.002 for concrete strength under 28 MPa and 0.003 for concrete strength over 82 MPa and is determined as a linear function of the concrete strength between 28 and 82 MPa (Tomii and Sakino, 1979). . The parts AB, BC, CD of the stress-strain curve for confined concrete depicted in Figure 2 are defined as follows:

$$\sigma_c = \left.\begin{matrix} f_c^{'} \\ \alpha f_c^{'} + 100(0.015-\varepsilon_c)(1-\alpha) f_c^{'} \\ \alpha f_c^{'} \end{matrix}\right\} \begin{matrix} \text{for } \varepsilon_c^{'} < \varepsilon_c \le 0.005 \\ \text{for } 0.005 < \varepsilon_c \le 0.015 \\ \text{for } \varepsilon_c > 0.015 \end{matrix} \tag{4}$$

where α is taken as 1.0 when the width-to-thickness ratio (*B/t*) of the composite column is less than 24 and is taken as 0.0 when the *B/t* ratio is greater than 64 as suggested by (Tomii and Sakino, 1979). For *B/t* ratios between 24 and 64, α is taken as 0.6 in the fiber element analysis program.

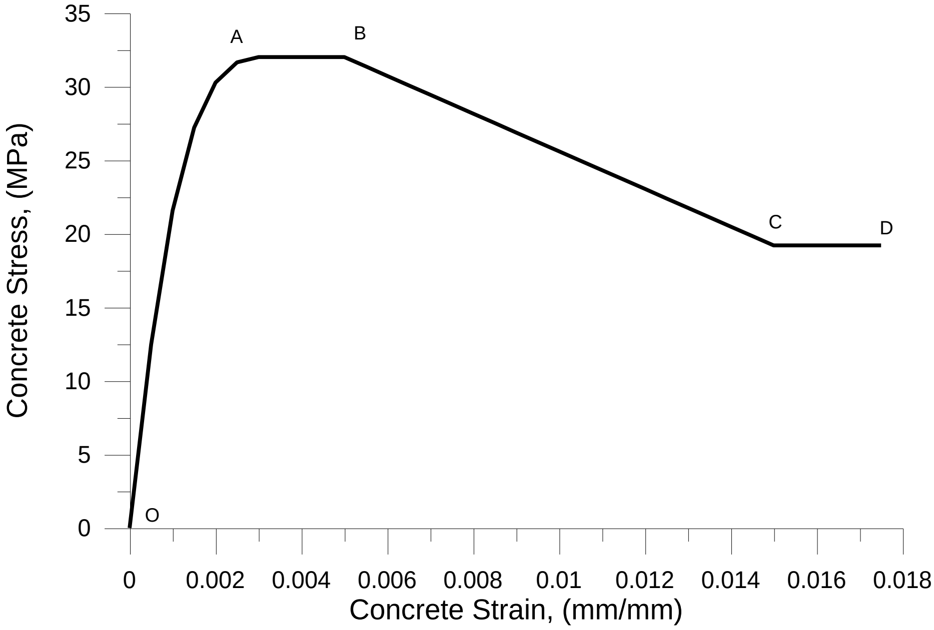

Figure (2): The Stress-Strain Curve for Confined Concrete.

2.3 Inelastic (Plastic) Buckling of Plates

For a rectangular plate of dimensions ($a \times b \times t$), which is loaded by membrane force, when the critical stress (σ_{cr}) exceed the proportional limit (σ_p), the buckling behavior of plate can be extended to the inelastic (plastic) range by using a reduced modulus of elasticity. However, the reduced modulus is not the tangent modulus. This is because the plate is anisotropic in its resistance to buckling at stresses exceeding the proportional limit (the double modulus theory), ($\sigma_y \ge \sigma_p$ and $0 < \sigma_x < \sigma_p$)

According to that the critical buckling stress is:

$$\sigma_{cr} = \frac{k\pi^2 E_r}{12(1-\nu^2)\left(\frac{b}{t}\right)^2} = \frac{\pi^2(\alpha^2+1)^2 E_r}{12(1-\nu^2)\left(\frac{a}{t}\right)^2} \tag{5}$$

where $\alpha = \dfrac{a}{b}$ the plate aspect ratio.

Here in this study unfilled steel tube in the mode shape of buckling shown in Figure (3), assume that ($\alpha = 1$), then the following equation can be obtained

$$\sigma_{cr} = \frac{4\pi^2 E_r}{12(1-\nu^2)\left(\frac{a}{t}\right)^2} \tag{6}$$

and

$$E_r = \frac{4EE_t}{\left(\sqrt{E} + \sqrt{E_t}\right)^2} \tag{7}$$

The reduced modulus of elasticity E_r depends mainly on the critical stress level E_t, thus the behavior is nonlinear and the method of trial and error is suggest to evaluate the accurate critical buckling stress at the plastic stage.

The interaction between concrete and steel behavior in concrete-filled box column, will reduce the effective plate aspect ratio as follows:

At initial stages;

$$\alpha_c = \frac{a}{\varepsilon_c b} \tag{8}$$

This equation yields large values of critical stresses after substituting into equation (5), and hence the yield stress will control the stresses in steel plate. Any successive increase in the applied load will be carried by concrete, until crushing occurs in concrete. The concrete will crack as vertical fibers. This is due to the lateral confinement of concrete by the shell of the steel box section. Then:

$$\alpha_{cp} \cong \frac{a}{\varepsilon_{cp} b + \beta \frac{b}{2}} \tag{9}$$

where β is the shear retention factor along the cracks. (i.e. β=1.0 for fully open cracks).

2.4 Geometric Imperfections and Residual Stresses

The initial out-of-plane imperfections, which induced during the processes of manufacture, welding and construction is considered. This initial buckles, affect the magnitude of lateral deformations under applied load. The initial geometric imperfections primarily influence the plate stiffness and become more obvious with an increased in the plate slenderness. The initial geometric imperfection that has the same mode shape of local buckling mode is considered in the analysis as illustrated in Figure 3.

The process of welding causes a complex state of temperature and stresses distribution with time in the welded steel plate. Tensile residual stresses are induced in the region of the weld, whilst compressive residual stresses are presented in the reminder of plate. The tensile stress at the welded edge reaches the yield stress of the steel plate. An idealized residual stress pattern in CFST column is shown in Figure 3. Residual stresses have been treated as a pre-load that is combined with the applied edge stresses in the analysis.

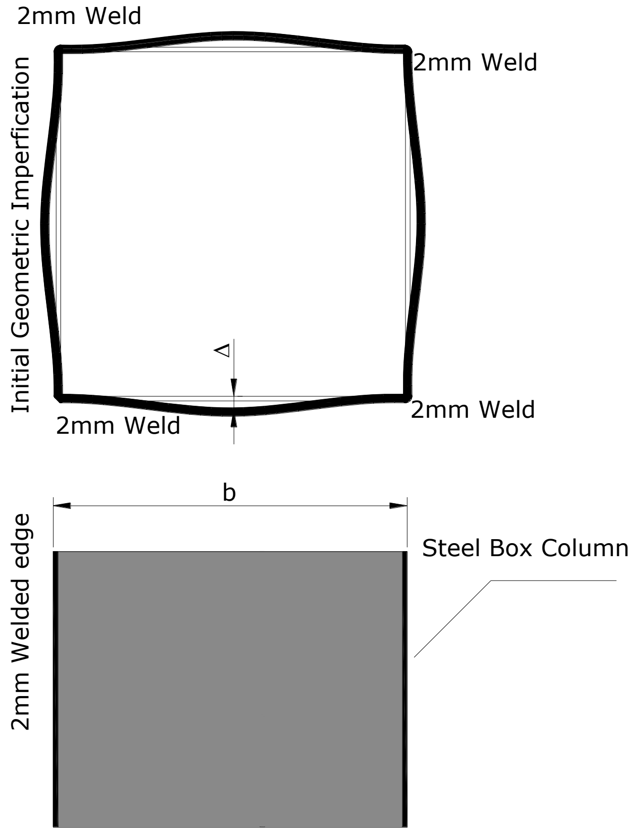

Figure (3): The Initial Out-of-Plane Geometric Imperforations.

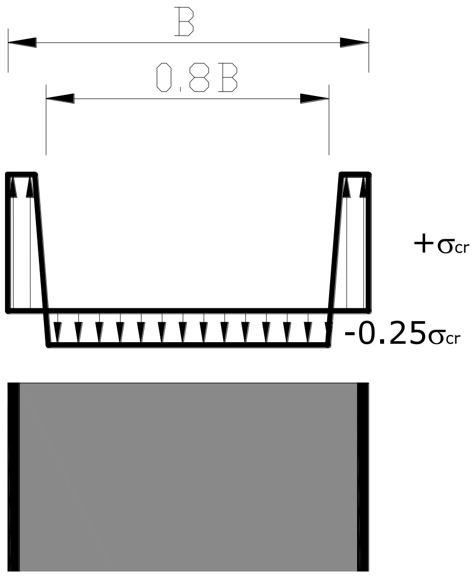

Figure (4): Distribution of Residual Stresses in Welded Steel Plate.

The stress-strain curve of the welded steel plate is no longer analogous to that of tensile test coupon without residual stresses. A typical material stress-strain curve of a welded steel plate with residual stresses displays a rounded stress-strain form.

2.5 The Effective Width Concept

The effective width concept is usually used to express the post-local buckling strength of thin steel plates. An effective width formula proposed by (Liang *et al.*, 2004) is improved herein numerically by using the fiber element analysis program and it is expressed by the following equation.

$$\frac{b_e}{b} = 0.861 + 4.318\times10^{-3}\left(\frac{b}{t}\right) - 1.097\times10^{-4}\left(\frac{b}{t}\right)^2 + 4.1203\times10^{-7}\left(\frac{b}{t}\right)^3 \qquad (10)$$

The previous effective width formula represents the state of the effective width at the ultimate load of CFST column. If it is required to trace the load deflection curve the following effective width equation is suggested (adopted from the numerical procedure presented by (Usami, 1982).

The computational procedure is outlined as follows:

1. Compute the maximum CFST column P_m.
2. Determine $P_i = 0.1(i-1).P_m$, where i= 1, 2,.., 11.
3. calculate $\left(\frac{\sigma_m}{\sigma_y}\right)$ from the following equations:

$$\left(\frac{\sigma_m}{\sigma_y}\right) = \frac{1}{2\lambda}\left(\beta - \sqrt{\beta^2 - 4\lambda}\right) \qquad (11)$$

(12)

$$\lambda = \sqrt{\frac{\sigma_y}{\sigma_{cr}}} \qquad (13)$$

$$\beta = 1 + C(\lambda - \lambda_o) + \lambda$$

$$\lambda_o = A - B.\ln\left(\frac{\Delta}{b}\right) \le 1.0 \qquad (14)$$

$$A = -0.05\left(1 - 10.84e^{-11.9\left(\frac{\sigma_{rc}}{\sigma_y}\right)}\right) \qquad (15)$$

(16)

$$B = 0.09\left(1 + 1.19e^{-12.4\left(\frac{\sigma_{rc}}{\sigma_y}\right)}\right) \qquad (17)$$

$$C = -157\left(\frac{\sigma_{rc}}{\sigma_y}\right)\left(\frac{\Delta}{b}\right) + 43\left(\frac{\Delta}{b}\right) + 1.2\left(\frac{\sigma_{rc}}{\sigma_y}\right) + 0.03$$

This procedure is applicable only in the following range [11]

$$0 \le \left(\frac{\sigma_{rc}}{\sigma_y}\right) \le 0.5, \quad \text{and} \quad \frac{1}{3233} \le \left(\frac{\Delta}{b}\right) \le \frac{1}{150} \qquad (18)$$

2.6 Section and Ductility Performance

In the (LRFD , 1999), a column is classified as composite if it has a structural steel area to the cross sectional area ratio of more than 0.04 otherwise it is treated as a concrete column. In (Eurocode 4 [1], the steel contribution ratio in a composite column section, which is defined as the ratio of the steel section strength to the composite section strength, must be greater than 0.2. To evaluate the section performance of composite columns, a performance index was proposed by [7] as:

$$PI_s = \frac{\sum_{i=1}^{Ns} \sigma_u^i A_s^i}{\sum_{i=1}^{Ns} \sigma_u^i A_s^i + \sum_{j=1}^{Nc} \sigma_u^j A_c^j} \qquad (10)$$

where σ_u^i is the longitudinal stress of steel fiber *i* at the ultimate load and σ_u^j the longitudinal stress of concrete fiber *j* at the ultimate load. The section performance index accounts for the effects of cross-sectional areas and material strengths of steel and concrete and b/t ratios.

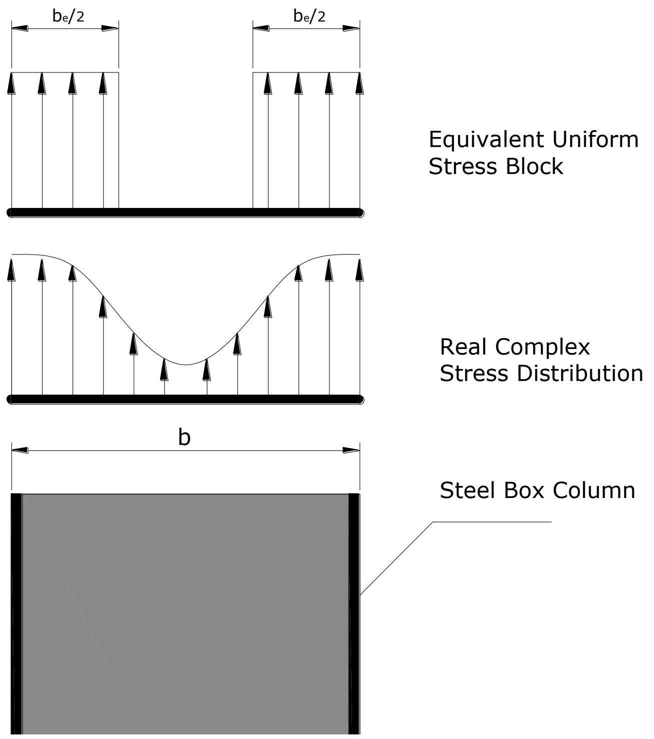

Figure (5): Distribution of Actual Stresses and Effective Width Concept.

To evaluate the axial ductility performance of CFST columns, the ductility performance index is defined as

$$PI_d = \frac{\varepsilon_{0.95}}{\varepsilon_y} \qquad (11)$$

where $\varepsilon_{0.95}$ is the axial strain when the load reach to 95% of the ultimate load and ε_y is the axial strain when the composite section is at yield.

3. Test Setup (Experimental Part)

3.1 Description

Buckling tests on six specimens made of low strength steel were presented herein. The yield stress of this grade was measured to be 250 MPa. The specimens were of stub column type with a box shaped cross section, Figure 6, and the height of the specimens was chosen to be 2.0 times the specimen width. This to prevent column buckling, avoid clamping effects from the end supports and to allow the specimen to buckle in such a way that the lowest buckling load would be acquired (as shown in Figure 7). Furthermore, the specimens were tested in as-welded condition. Two specimens were tested without concrete filling (SP5 and SP6), while the other four specimens are filled with concrete with different compressive strength. (SP1 and SP2) were filled with concrete having compressive strength about 32 MPa, while the specimen (SP3 and SP4) were filled with concrete of 45 MPa compressive strength.

Figure (6): Specimen layout and weld detailing.

The tests were performed at the Strength of Materials Laboratory in the College of Engineering at Babylon University. The specimens were subjected to uniaxial compression load by placing the specimens between two rigid end plates. The deformation speed was chosen such that the nominal stress would reach the yield strength within 30 seconds. Furthermore the deformations of the specimens were carried on until a 50% load drop from the ultimate load was acquired (Figure 8).

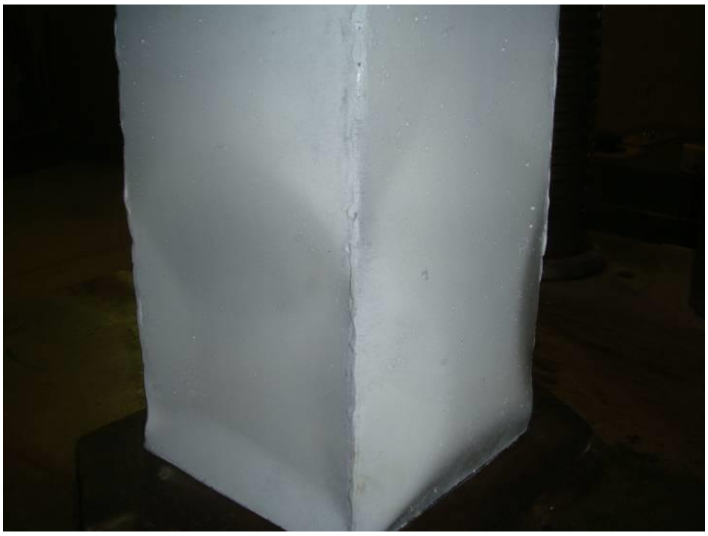

a) Experimental Buckling Mode.

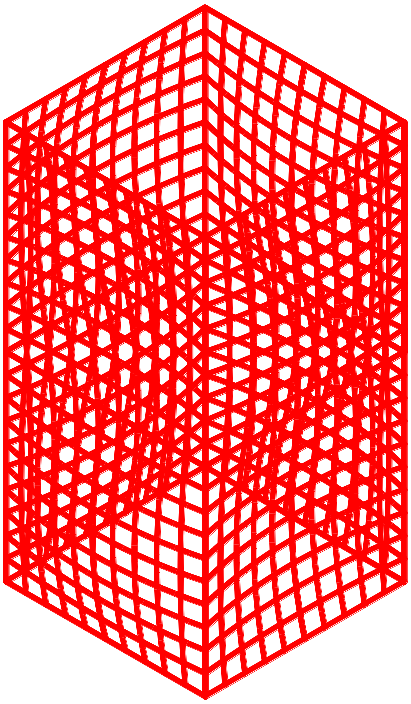

b) Theoretical Finite Element Analysis (the lowest mode shape).

Figure (7): The Post-Buckled Shape of Specimen *SP5* and *SP6*.

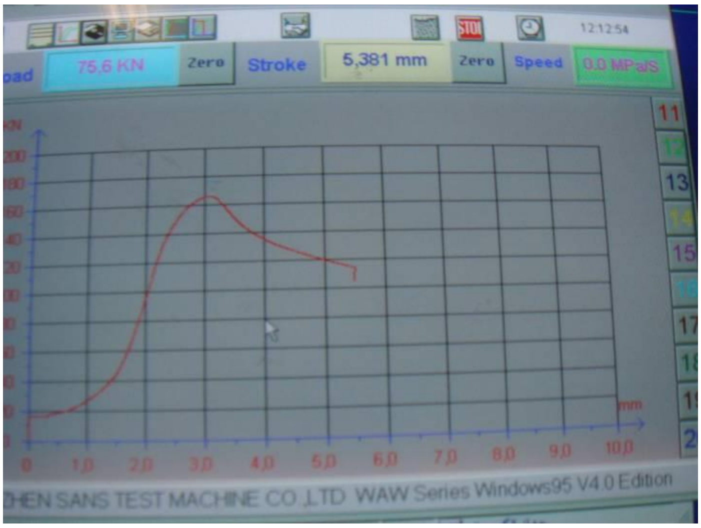

Figure (8): The Load Deflection curve of Specimen *SP5*.

Deformation and load data was sampled during the tests for specimens have an ultimate testing load less than the maximum permissible load of the testing machine; i.e. 1000 kN. The specimens with high compressive strength (SP3 and SP4) were tested at the Laboratories of Karbala Company for Fabricating Precast Buildings. Only the ultimate load capacity of the specimens were evaluated not their deformation (Figure 9).

Figure (9): Apparatus Recording the Ultimate Load Capacity of Specimen *SP3*.

3.2 Test Results and Comparisons

The test results are evaluated with respect to the theoretical finite element analysis.

Regarding the presented results collected through the test results are of great importance to be used as a reference.

The results are listed in Table 1. Comparisons between the theoretical and experimental data are listed also. A comparison between the load-edge shorting is depicted in Figure 10.

Table (1): Test Data and Results

Specimen Designation	Type	Dimensions $(h \times b \times t)$ (mm).	Concrete strength f_{cu}, (MPa).	Edge shorting at peak Load, (mm).	Peak load, (kN).		Abs. Diff. %
					Experimental	Theoretical	
SP-1-C40	CFST	300x150x2	32	1.2	932	870	6.6%
SP-2-C40*	CFST	300x150x2	34	1.25	882	870	1.4%
SP-3 –C60	CFST	300x150x2	45	1.31	1294	1315	1.6%
SP-4-C60	CFST	300x150x2	44.5	1.29	1275	1315	3.1%
SP-5	ST	300x150x2	-	3.2	174	154	11.5%
SP-6	ST	300x150x2	-	3.5	182	154	15.3%

At failure the concrete crushed in many directions (random orientations), the concrete still has the ability to resist axial loads, which is a very important feature in seismic resisting structures (Figure 11 shows failed CFST column). Due to the concrete fixity to the steel plate, buckling will occur at the final stages. Also the slenderness ratio of the plate is small and increased with the increase of the amount of concrete crashing.

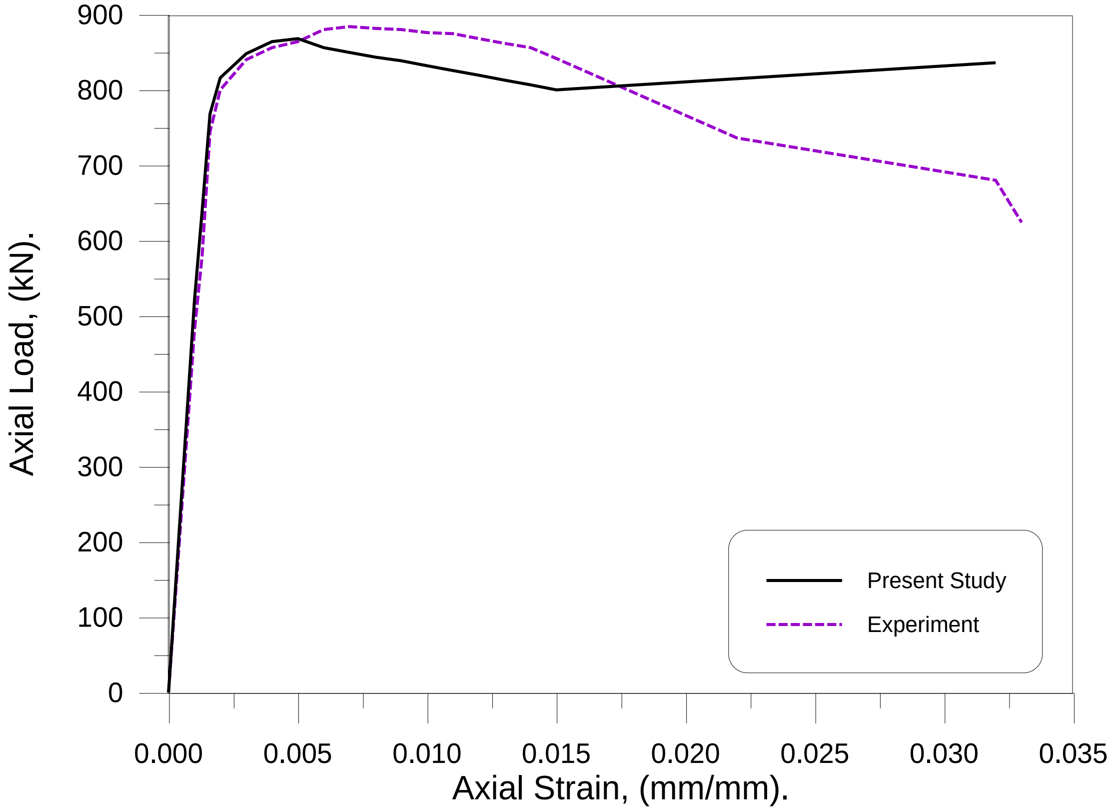

Figure (10): Comparison of the present study versus experimental results (Specimen SP2-C40*).

Figure (11): Failure Pattern of CFST column (Specimen SP3-C60).

4. Conclusions

In this paper, the ultimate strength and ductility of short concrete-filled thin-walled steel box columns have been investigated using the fiber element analysis technique. The progressive local and post-local buckling of a thin-walled CFST column is modeled by gradually distributing the normal stresses within the steel box. The elastic and plastic effective width concept is employed herein. The effect of initial geometric imperfection and residual stresses are considered in the analysis by presenting formulas for the effective width of CFST columns. The filling concrete will enhanced the steel carrying capacity so that all the section will reach its limit state and avoid the possibility of buckling until cracking induced in concrete at high load levels. At the same time the steel shell will confine the concrete and improve its strength and ductility. The steel column with steel ratio about 2% will increase the composite column capacity by about (15%-21%)

5. Acknowledgment

Special thanks awarded to the employers of the Laboratories of College on Engineering/ Strength of Materials Laboratory and Karbala Company for Fabricated Precast Building workshops and their Laboratories.

References

ACI 318-05. (2005). Building code requirements for reinforced concrete. ACI, Detroit, MI, USA.

Bridge, R.Q., O'Shea, M.D., Gardner, P., Grigson, R. and Tyrell, J., (1995). "*Local buckling of square thin-walled steel tubes with concrete infill*". Proc. of the Int. Conf. on Structural Stability and Design, Sydney, Australia, pp. 307-314.

El-Tawil, S. and Deierlein, G.G., (1999). "*Strength and ductility of concrete encased composite columns*". Journal of Structural Engineering, ASCE, Vol. 125, No. 9, pp. 1009-1019.

El-Tawil, S., Sanz-Picón, C.F. and Deierlein, G.G. (1995). "*Evaluation of ACI 318 and AISC (LRFD) strength provisions for composite beam-columns*". Journal of Constructional Steel Research, Vol. 34, No. 1, 103-126.

Eurocode 4. (1994). Design of composite steel and concrete structures, Part 1.1, general rules and rules for buildings. .

Ge, H.B. and Usami, T., (1992). "*Strength of concrete-filled thin-walled steel box columns: experiments*". Journal of Structural Engineering, ASCE, Vol.118, No. 11, pp. 3036-3054.

Lakshmi, B. and Shanmugam, N.E., (2002). "*Nonlinear analysis of in-filled steel-concrete composite columns*". Journal of Structural Engineering, ASCE, Vol. 128, No. 7, pp. 922-933.

Liang, Q.Q. and Uy, B., (2000) "*Theoretical study on the post-local buckling of steel plates in concrete filled box columns*". Computers and Structures, Vol. 75, No. 5, pp. 479-490.

Liang, Q.Q., (2007). "*Inelastic Behavior of Concrete-Filled Thin-Walled Steel Tubular Columns Subjected To Local Buckling"*, Journal of computer and structures, 2007 (submitted)

Liang, Q.Q., Uy, B. and Liew, J.Y.R., (2005). "*Local buckling of steel plates in concrete-filled thin walled steel tubular beam-columns*". Journal of Constructional Steel Research, (submitted).

Liang, Q.Q., Uy, B., Wright, H.D. and Bradford, M.A., (2004). "*Local buckling of steel plates in double skin composite panels under biaxial compression and shear*". Journal of Structural Engineering, ASCE, Vol. 130, No. 3, pp. 443-451.

Liew, J.Y.R., Chen, H. and Shanmugam, N.E., (2001). "*Inelastic analysis of steel frames with composite beams*". Journal of Structural Engineering, ASCE, Vol. 127, No. 2, pp. 194-202.

LRFD. (1999). Load and resistance factor design specification for steel buildings. American Institution of Steel Construction.

Mander, J.B., Priestly, M.N.J. and Park, R., (1988). "*Theoretical stress-strain model for confined concrete*". Journal of Structural Engineering, ASCE, Vol. 114, No. 8, pp. 1804-1826.

Nara, K., Kojima, H., Tsuda, M., and Komatsu, S., (1987). "A study on Characteristics of Ultimate Strength of Steel Plate with Initial Imperfections Under In-plane Bending and Compression", Proc., JSCE, 386/I-8, pp. 275-283. (Cited in Usami)

Ramberg, W. and Osgood, W.R., (1943). "*Description of stress-strain curves by three parameters*". NACA Technical Note. No. 902,(cited in 7)

Schneider, S.P., (1998). "*Axially loaded concrete-filled steel tubes*". Journal of Structural Engineering, ASCE, Vol. 124, No. 10, pp. 1125-1138.

Tomii, M. and Sakino, K., (1979). "*Elastic-plastic behavior of concrete filled square steel tubular beam columns*". Trans. Arch. Inst. Japan, Vol. 280, 1979, pp. 111-120.

Usami, T., (1982). " Post-buckling of plates in compression and bending." Journal of Structural Div., ASCE, Vol. 108 No.3, 1982, pp. 591-609.

Uy, B., (2000). "*Strength of concrete-filled steel box columns incorporating local buckling*". Journal of Structural Engineering, ASCE, Vol. 126, No. 3, pp. 341-352.